IEEE Photonics Journal
An IEEE Photonics Society Publication

Open Access

# Analysis of 270/290/330-nm AlGaN-Based Deep Ultraviolet Light-Emitting Diodes With Different Al Content in Quantum Wells and Barriers

Volume 7, Number 6, December 2015

G. F. Yang
Q. Zhang
J. Wang
S. M. Gao
R. Zhang
Y. D. Zheng

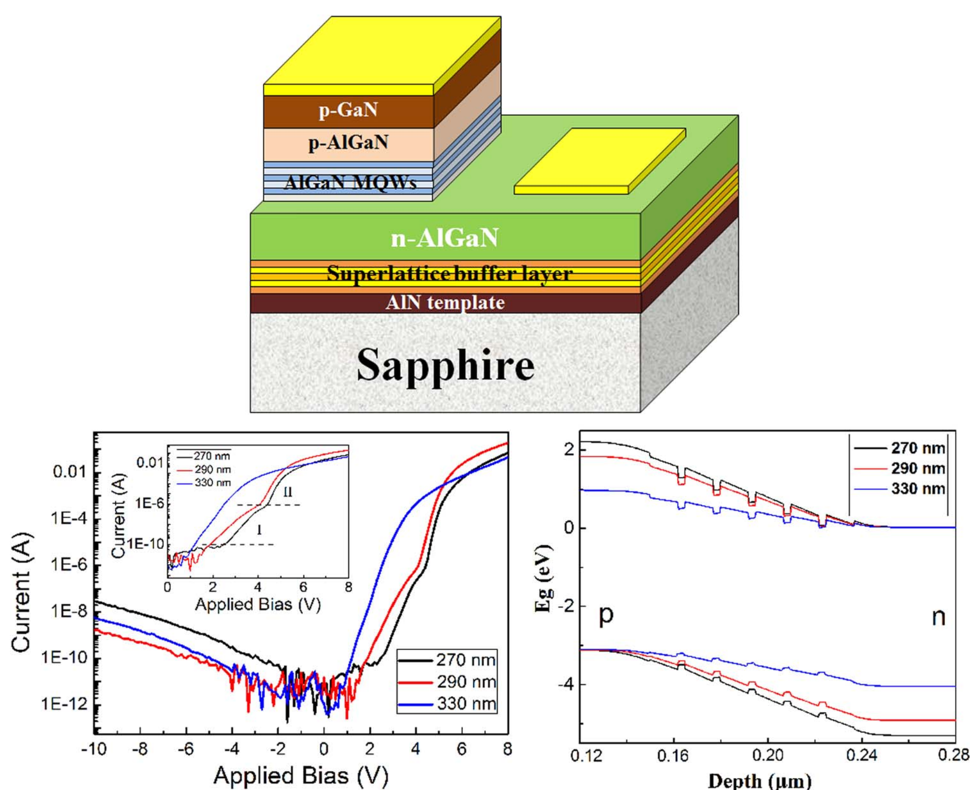


DOI: 10.1109/JPHOT.2015.2491604
1943-0655 © 2015 IEEE

IEEE photonics SOCIETY
IEEE

# Analysis of 270/290/330-nm AlGaN-Based Deep Ultraviolet Light-Emitting Diodes With Different Al Content in Quantum Wells and Barriers

**G. F. Yang,[1,2] Q. Zhang,[1] J. Wang,[1] S. M. Gao,[1] R. Zhang,[2] and Y. D. Zheng[2]**

[1]School of Science, Jiangsu Provincial Research Center of Light Industrial Optoelectronic Engineering and Technology, Jiangnan University, Wuxi 214122, China
[2]School of Electronic Science and Engineering, Nanjing University, Nanjing 210093, China

*DOI: 10.1109/JPHOT.2015.2491604*
*1943-0655 © 2015 IEEE. Translations and content mining are permitted for academic research only. Personal use is also permitted, but republication/redistribution requires IEEE permission. See http://www.ieee.org/publications_standards/publications/rights/index.html for more information.*

Manuscript received September 22, 2015; revised October 12, 2015; accepted October 13, 2015. Date of publication October 15, 2015; date of current version October 26, 2015. This work was supported in part by the Natural Science Foundation of Jiangsu Province (Nos. BK20150158, BK2011436, and BM2014402), by the China Postdoctoral Science Foundation (Nos. 2014M561623 and 2014M551559), by Jiangsu Planned Projects for Postdoctoral Research Funds (No. 1401013B), and by the Fundamental Research Funds for Central Universities (Nos. JUSRP51517 and JUSRP11408). Corresponding author: G. F. Yang (e-mail: gfyang@jiangnan.edu.cn).

**Abstract:** The optical and electrical properties of 270/290/330-nm AlGaN-based deep ultraviolet (UV) light-emitting diodes (LEDs) with different Al content in quantum wells and barriers have been investigated systematically. Based on the experimental and numerical study, it is observed that the UV LEDs with longer wavelength and lower Al composition in AlGaN multiple quantum wells (MQWs) possess less dislocation density, higher light output power, and external quantum efficiency. Large ideality factors calculated from the I–V curves and simulated energy band profiles indicate that the current in the deep UV LEDs with high Al content is dominated by tunneling mechanism, which is attributed to the resulting potential drop in the active region caused by large polarization field in AlGaN MQWs.

**Index Terms:** AlGaN, deep ultraviolet, light-emitting diodes (LEDs), numerical simulation.

## 1. Introduction

Deep ultraviolet light-emitting diodes (UV LEDs) based on high Al content AlxGa1-xN materials have been a subject of great interest due to their extensive applications, such as air and water purification, surface disinfection, UV curing, and medical phototherapy. Although the output power of deep UV LEDs have greatly increased [1]–[3], $Al_xGa_{1-x}N$ based deep UV LEDs still suffer from relatively low external quantum efficiency (EQE) and emission power [4]. The EQEs of the reported deep UV LEDs with emission wavelengths ranging from 200 to 350 nm are typically less than 10%, which are about one order of magnitude lower than those of LEDs in the near UV and visible spectral range based on InxGa1-xN materials [2]. The causes responsible for the low efficiency of $Al_xGa_{1-x}N$ deep UV LEDs are various. First, the increased Al content in $Al_xGa_{1-x}N$ materials would cause higher dislocation density when grown on sapphire substrates, inducing severe nonradiative recombination [5]. Second, the strong spontaneous and piezoelectric polarization charges induced at the interface of the active layers for III-nitride

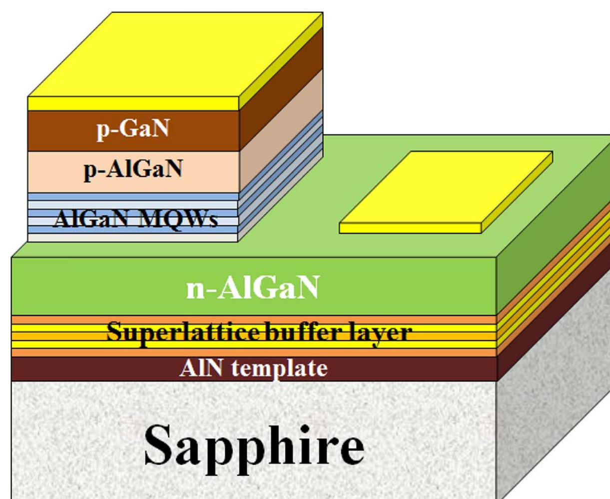


Fig. 1. Schematic diagram of the deep UV LEDs.

materials make the band diagrams of quantum wells (QWs) titled and result in reduced overlap of electron and hole wave functions, which further deteriorate the radiative recombination rate [6]. Besides, the strong electron leakage due to the large imbalance for hole and electron injection in deep UV LEDs is considered as an important factor reducing the internal quantum efficiency (IQE) [7]. To solve these issues, various energy band engineering methods [8]–[10], low-dislocation-density substrates, in combination with substrate thinning, encapsulation, and reflective electrodes have been utilized. However, it is often difficult to distinguish the contribution of each technology breakthrough to the internal and external quantum efficiencies, and the related mechanisms have not been completely understood yet.

In this study, in order to investigate the effect of Al composition varying in AlGaN MQWs on the optoelectronic properties of AlGaN-based deep UV LEDs, we have fabricated three deep UV LEDs emitting at 270, 290, and 330 nm by changing the Al content in the AlGaN quantum wells and barriers, while the other epilayers are kept in the same structure. The origin of the electroluminescence (EL), EQE and electrical performance of deep UV LEDs is investigated. Two-dimensional (2-D) numerical simulation is applied to explain the mechanisms for deep UV LEDs physically.

## 2. Experimental Details

Fig. 1 shows the schematic diagram of the fabricated deep UV LEDs. The LEDs were grown on basal plane sapphire substrates by metal–organic chemical vapor deposition (MOCVD). Trimethylgallium (TMGa), trimethylaluminium (TMAl), silane, Cp2-Mg, and ammonia ($NH^3$) were used as precursors, and the carrier gas was $H^2$. Following the high quality AlN template and AlN/AlGaN superlattice growth, a 2-$\mu$m-thick Si-doped ($N_D = 5 \times 10^{18}\text{cm}^{-3}$) n-type AlGaN layer and active region, which consisted of 5 periods $Al_xGa_{1-x}N/Al_yGa_{1-y}N$ multiple quantum wells (MQWs) with the well and barrier thickness of 3 and 12 nm, respectively, were grown in sequence. The growth temperatures of AlN and AlGaN layers are around 1100 °C–1200 °C with a reactor pressure of 70 mbar and $NH^3$ flow of 1000 SCCM (SCCM denotes standard cubic centimeter per minute). For the $Al_xGa_{1-x}N$ QW layers, the TMAl flow of three LEDs was kept the same at 160 SCCM, while the TMGa flows were 50, 58, and 72 SCCM for the 270, 290, and 330 nm UV LEDs, respectively. When growing the $Al_yGa_{1-y}N$ quantum barrier layers, the TMAl flow of three LEDs was kept the same at 200 SCCM, while the TMGa flows were 47, 53, and 68 SCCM for the 270, 290, and 330 nm UV LEDs, respectively. Finally, the MQW region was capped by 50 nm p-AlGaN and 100 nm p-GaN layers. As for the 270/290/330 nm UV emissions,

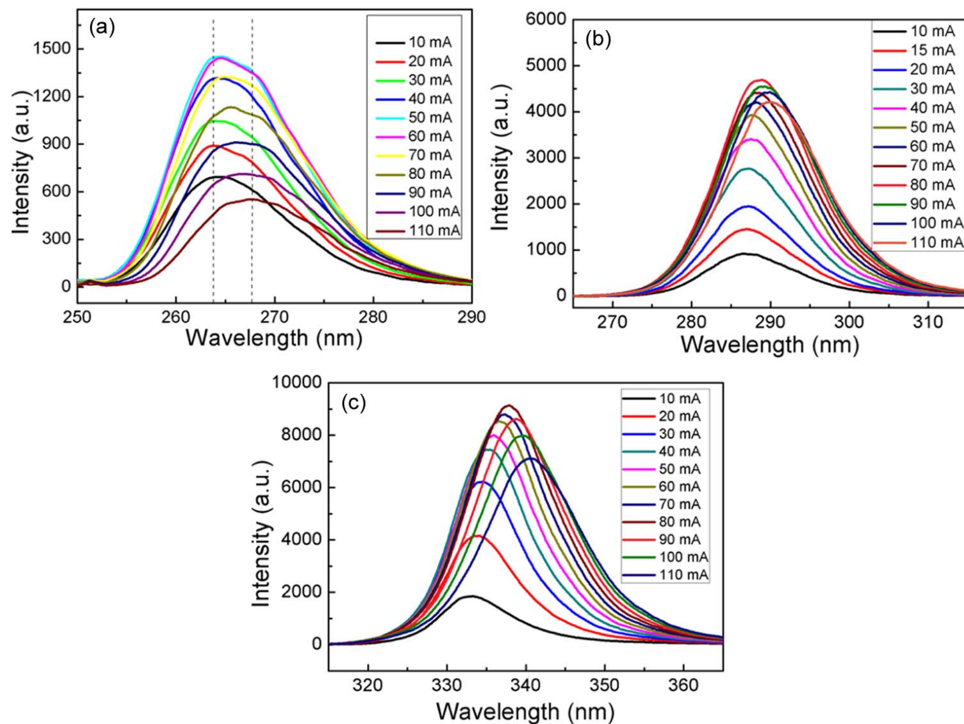


Fig. 2. EL spectra as a function of injection current for 270 nm (a), 290 nm (b), and 330 nm (c) UV LEDs.

the Al compositions in the well layers were set as $x = 0.6/0.5/0.15$, and the Al compositions in the well layers were set as $y = 0.7/0.6/0.25$, respectively.

$300 \times 300\ \mu m^2$ mesa type LED devices were fabricated by using standard photolithography and dry etching process to access the bottom n-AlGaN layer. The Ti/Al/Ti/Au n-type ohmic contact metallization was annealed at 950°C, and semitransparent current spreading Ni/Au metals were deposited on p-GaN. The EL spectra, current-voltage (I-V) curve, and output powers of the LEDs were obtained using a probe station with photo detectors.

## 3. Results and Discussion

Fig. 2 shows the EL spectra of 270/290/330 nm deep UV LEDs as a function of injection current. It can be clearly seen that the 270 nm LED reveals a broader full-width-at-half-maximum (FWHM) of about 16 nm, which is larger than the FWHM value of about 11 nm for the 290 and 330 nm LED at 20 mA injection current. Furthermore, the EL spectra of 270 nm LED shows the main emission peak with a weak parasitic peak at the right side of the main peak, while only one uniform emission peak is observed for both 290 and 330 nm LEDs. These results would be due to the potential fluctuations caused by alloy composition or well width variation in AlGaN QWs, as phase separation can be easily occurred during the growth of AlGaN with high Al content. The lateral phase often occurs due to nonuniform growth and different mobility of Al and Ga adatoms. Islands, pyramids, and V-type trenches form during initial growth of and AlGaN layer [11]. On the other hand, there is a blue-shift of the emission peaks with increasing current at shorter wavelengths, which is attributed to the banding filling of localized states and screening of the piezoelectric field in the QWs with higher Al content, and the EL emission peaks of the three UV LEDs also show a red shift as the injection current increased, indicating the strong self-heating effect under continuous wave (CW) injection current mode [12].

Fig. 3(a) and (b) show the current-output (I-L) and normalized EQE characteristics of the 270/290/330 nm LEDs. The I-L curve is linear at low currents but becomes sublinear and

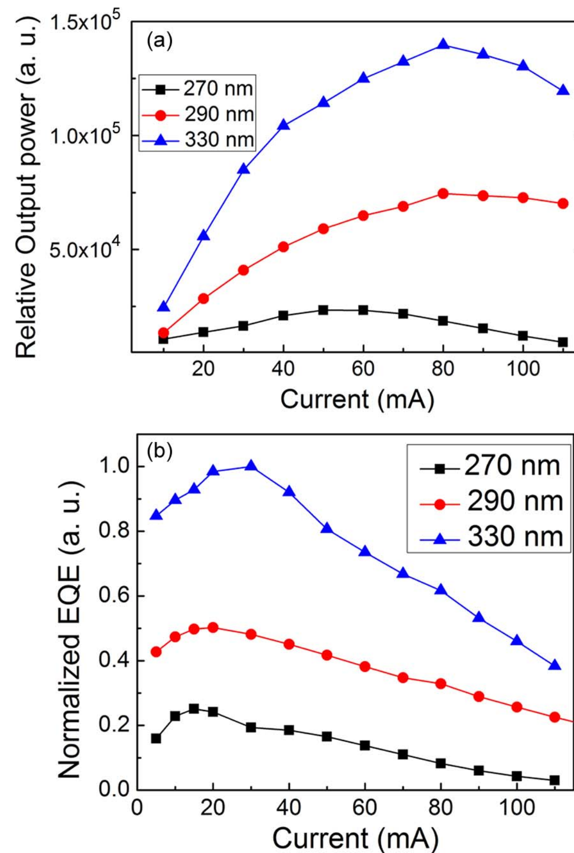


Fig. 3. Current-dependent output power (a) and normalized EQE (b) of the three deep UV LEDs.

decreased at high currents, indicating a reduced EQE, which is attributed to the self-heating thermal effect in the UV LEDs. Moreover, as can be seen from Fig. 3, it is evident that the light output power and EQE are increased as the Al content in the quantum well and barrier layers reduced for 270/290/330 nm LEDs. This is because the increased Al content in $Al_xGa_{1-x}N$ materials would cause higher dislocation density when grown on sapphire substrates, inducing severe nonradiative recombination centers [13]. It is also noteworthy that the maximum EQE of 330 nm LED is much larger than that of 270 and 290 nm LEDs. The extraction efficiency of AlGaN-based deep UV LEDs would be influenced by the UV light absorption in the p-GaN contact layer, and the unique optical polarization properties. As the design of the p-GaN layer for the three LEDs is the same, the extraction efficiency would be mainly affected by the optical polarization effect. For AlGaN-based LEDs, the polarization of light changes from transverse-electric (TE) to the transverse-magnetic (TM) polarized mode as the Al composition increases or the wavelengths decreases, and the light extraction efficiency of the TM-polarized light is much lower than that of the TE-polarized light, therefore, the efficiency reduces at shorter wavelengths [14]. The current that EQE reached maximum in 330 nm LED is higher than that in 270 and 290 nm LEDs. After reaching the maximum values, the EQE of the three LEDs decrease with the increased injection current owing to carrier spillover from the QWs into the barrier layers, which is originated from energy band bending caused by strong polarization field in AlGaN QWs.

The current-voltage (I-V) characteristics of the 270/290/330 nm LEDs are shown in Fig. 4. The forward voltages of the 270, 290, and 330 nm LEDs are, respectively, 5.3, 5, and 4.5 V at the injection current of 5 mA, indicating the electrical property could be deteriorated as the Al content in the AlGaN MQWs increased. Due to the high activation energies of Mg in high Al content AlxGa1-xN materials, the hole concentration is very low, leading to a large resistivity [15]. It

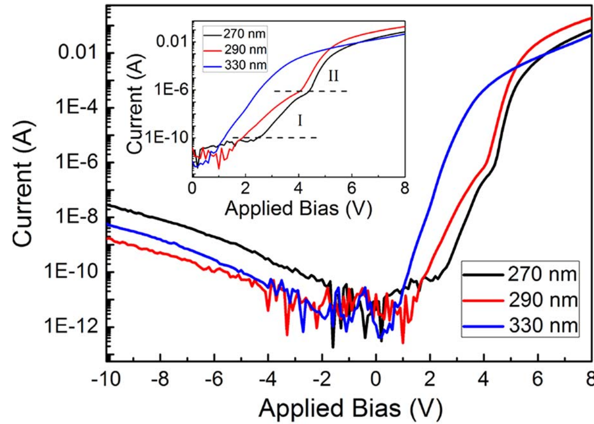


Fig. 4. I-V curves of the three deep UV LEDs at room temperature. (Inset) Corresponding forward I-V curves.

is also noted that the behavior of the I-V characteristics reveals obvious difference the 330 nm LED and the other two UV LEDs at moderate forward voltages ($2\leqslant V\leqslant 6$). As for the 270 and 290 nm UV LEDs, two different exponential segments are clearly seen within moderate forward voltage, which are indicated as region I and II in the inset of Fig. 4. While only one exponential segment appears for the 330 nm LED within the same moderate voltage range. The ideality factor n of the LEDs at moderate voltage can be expressed using the following equation:

$$I-\frac{V}{R_P}=I_s\exp\left\{\frac{q[V(1+R_s/R_P)-IR_S]}{nkT}\right\} \tag{1}$$

where $R_P$ is parallel resistance, $R_s$ is series resistance, $I_s$ is the saturation current, $k$ is the Boltzmann constant, and $T$ is the absolute temperature [16]. For the AlGaN-based deep UV LEDs, the values of the parallel resistance RP are in the order of $10^{11}$, which is several orders larger than the value of $R_s$, thus the numerical terms of $V/R_p$ and $R_s/R_p$ can be ignored when calculating the ideality factor, and (1) is simplified as

$$\frac{dV}{dI}=R_S+\frac{nkT}{qI}. \tag{2}$$

The ideality factors in region I are calculated as 8.01, 7.8, and 5 for the 270, 290, and 330 nm LEDs, respectively. In region II, the ideality factors are 4.05 and 3.92 for 270 and 290 nm LEDs, respectively. All of the ideality factors are much larger than 2, the large ideality factor cannot be explained by Shockley diffusion and recombination mode, indicating the presence of a significant current tunneling process in the three LEDs at moderate forward bias voltage. It is noted that the ideality factor decreases as the Al composition in the AlGaN MQWs is reduced, which is attributed to the higher dislocation density in $Al_xGa_{1-x}N$ materials with increased Al content [17].

In order to understand the optoelectronic properties and investigate the origin of large tunneling current in the deep UV LEDs physically, the energy band diagrams of the 270/290/330 nm UV LEDs are calculated by 2-D numerical simulations using Silvaco Atlas software, shown in Fig. 5. In the simulation, both the band offset ratios of AlGaN/AlGaN and AlGaN/GaN are set to be 0.5/0.5 according to the report of Piprek *et al.* [18]. The incomplete ionization model in the software has been used to calculate the ionized electron and hole concentrations. Poisson's equation and carrier continuity equation are applied with carrier concentration dependent mobility model, field dependent mobility model, Shockley-Read-Hall (SRH) recombination model, surface recombination model, Auger recombination model, and optical generation-recombination taken into account [19]. According to the mechanism reported by Fiorentini *et al.* [20], the

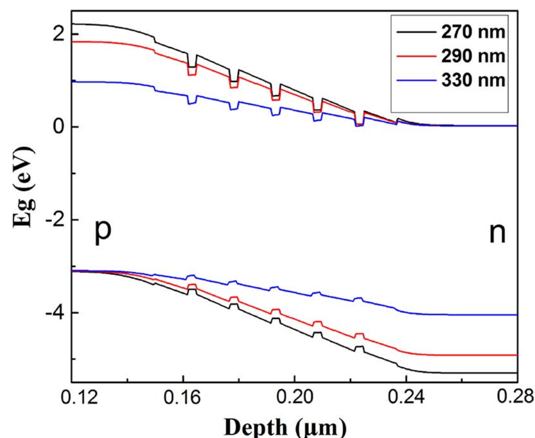


Fig. 5. Energy band diagrams for 270, 290, and 330 nm UV LEDs at forward voltage of 4 V calculated by 2-D numerical simulations.

polarization effect of wurtzite $Al_xGa_{1-x}N$ alloy is considered with 50% of the polarization charges compensated by defects and interface charges. The detailed parameters used in the simulation could be found in Ref. [21]. As can be seen from Fig. 5, when 4 V forward voltage is applied, the energy band diagrams of 270 and 290 nm LEDs exhibit large potential drop from the p-type to n-type side. In contrast, 330 nm LED shows a flatter potential drop in the same region when compared with that of 270 and 290 nm LEDs. This is because the difference of Al content in $Al_xGa_{1-x}N$ materials induces different polarization filed in the active region, and cause different degrees of energy band banding. The large potential drop is considered to act as a barrier for the electron and hole injection, which would reduce the light output power and EQE of LEDs and can explain the results shown in Figs. 2 and 3. Furthermore, the diffusion current is believed to be suppressed by the potential barrier, and the total current is dominated by tunneling current in the active region through trap levels in the forbidden band gap for the 280 and 250 nm LEDs.

## 4. Conclusion

In conclusion, we have investigated the effects of different Al content in AlGaN MQWs on the optical and electrical characteristics of AlGaN-based deep UV LEDs. The LEDs with high Al content in AlGaN MQWs suffer from low light output power and external quantum efficiency, which results from the reduced material quality with large dislocation density and the optical polarization effect. The red shift of the peak wavelength has been obviously observed as the injection current increases, which is due to the strong self-heating thermal effect under CW operation mode. Large ideality factors are obtained from the I-V curves of the deep UV LEDs, indicating the presence of a significant current tunneling process. These experimental findings are reproduced by energy band structure calculations using 2-D numerical simulation and can be explained by the different degrees of band bending and polarization field in the MQWs.

## References

[1] M. Shatalov *et al.*, "Efficiency of light emission in high aluminum content AlGaN quantum wells," *J. Appl. Phys.*, vol. 105, no. 7, 2009, Art. ID. 073103.
[2] A. Khan, K. Balakrishnan, and T. Katona, "Ultraviolet light-emitting diodes based on group three nitrides," *Nat. photon.*, vol. 2, no. 2, pp. 77–84, 2008.
[3] A. J. Fischer *et al.*, "Room-temperature direct current operation of 290 nm light-emitting diodes with milliwatt power levels," *Appl. Phys. Lett.*, vol. 84, no. 17, pp. 3394–3396, 2004.
[4] M. Shatalov *et al.*, "AlGaN deep-ultraviolet light-emitting diodes with external quantum efficiency above 10%," *Appl. Phys. Exp.*, vol. 5, no. 8, 2012, Art. ID. 082101.

[5] H. Hirayama, T. Yatabe, N. Noguchi, T. Ohashi, and N. Kamata, "231-261 nm AlGaN deep-ultraviolet light-emitting diodes fabricated on AlN multilayer buffers grown by ammonia pulse-flow method on sapphire," *Appl. Phys. Lett.*, vol. 91, no. 7, 2007, Art. ID. 071901.

[6] M.-F. Huang and T.-H. Lu, "Optimization of the active-layer structure for the deep-UV AlGaN light-emitting diodes," *IEEE J. Quantum Electron.*, vol. 42, no. 8, pp. 820–826, Aug. 2006.

[7] K. H. Kim *et al.*, "AlGaN-based ultraviolet light-emitting diodes grown on AlN epilayers," *Appl. Phys. Lett.*, vol. 85, no. 20, pp. 4777–4779, 2004.

[8] M. F. Schubert *et al.*, "Polarization-matched GaInN/AlGaInN multi-quantum-well light-emitting diodes with reduced efficiency droop," *Appl. Phys. Lett.*, vol. 93, no. 4, 2008, Art. ID. 041102.

[9] J. C. Zhang *et al.*, "Suppression of the subband parasitic peak by 1 nm i-AlN interlayer in AlGaN deep ultraviolet light-emitting diodes," *Appl. Phys. Lett.*, vol. 93, no. 13, 2008, Art. ID. 131117.

[10] R. Gutt *et al.*, "AlGaN based 355 nm UV light-emitting diodes with high power efficiency," *Appl. Phys. Exp.*, vol. 5, no. 3, 2012, Art. ID. 032101.

[11] M. Gherasimova *et al.*, "Heteroepitaxial evolution of AlN on GaN grown by metal-organic chemical vapor deposition," *J. Appl. Phys.*, vol. 95, no. 5, pp. 2921–2923, 2004.

[12] Y. Yang, X. A. Cao, and C. H. Yan, "Investigation of the nonthermal mechanism of efficiency rolloff in InGaN light-emitting diodes," *IEEE Trans. Electron Devices*, vol. 55, no. 7, pp. 1771–1775, Jul. 2008.

[13] K. X. Chen *et al.*, "Effect of dislocation on electrical and optical properties of n-type $Al_{0.34}Ga_{0.66}N$," *Appl. Phys. Lett.*, vol. 93, no. 19, 2008, Art. ID. 192108.

[14] H. Y. Ryu, I. G. Choi, H. S. Choi, and J. I. Shim, "Investigation of light extraction efficiency in AlGaN deep-ultraviolet light-emitting diodes," *Appl. Phys. Exp.*, vol. 6, no. 6, 2013, Art. ID. 062101.

[15] Y. Li *et al.*, "Advantages of AlGaN-based 310 nm UV light-emitting diodes with Al content graded AlGaN electron blocking layers," *IEEE Photon. J.*, vol. 5, no. 4, 2013, Art. ID. 8200309.

[16] H. Witte *et al.*, "Electrical investigation of AlGaN/AlN structures for LEDs on Si (111)," *Phys. Status Solidi A*, vol. 208, no. 7, pp. 1597–1599, 2011.

[17] K. B. Lee *et al.*, "The origin of the high ideality factor in AlGaN-based quantum well ultraviolet light emitting diodes," *Phys. Status Solidi B*, vol. 247, no. 7, pp. 1761–1763, 2010.

[18] J. Piprek and S. Li, "Electron leakage effects on GaN-based light-emitting diodes," *Opt. Quantum Electron.*, vol. 42, no. 2, pp. 89–95, 2010.

[19] G. F. Yang, G. H. Li, S. M. Gao, D. W. Yan, and F. X. Wang, "Characteristics of N-face InGaN light-emitting diodes with p-type InGaN/GaN superlattice," *IEEE Photon. Technol. Lett.*, vol. 25, no. 23, pp. 2369–2372, Dec. 2013.

[20] V. Fiorentini, F. Bemardini, F. D. Sala, A. D. Carlo, and P. Lugli, "Effect of macroscopic polarization in III-V nitride multiple quantum wells," *Phys. Rev. B, Condens. Matter*, vol. 60, no. 12, pp. 8849–8858, 1999.

[21] I. Vurgaftman, J. R. Meyer, and L. R. Ram-Mohan, "Band parameters for III-V compound semiconductors and their alloys," *J. Appl. Phys.*, vol. 89, no. 11, pp. 5815–5875, 2001.